Proceedings of
ASME TURBO EXPO 2002
June 3-6, 2002, Amsterdam, The Netherlands

GT-2002-30629

EVALUATION OF MECHANICAL RELIABILITY OF SILICON NITRIDE VANES AFTER FIELD TESTS IN AN INDUSTRIAL GAS TURBINE

H.-T. Lin and M. K. Ferber
Metals and Ceramics Division
Oak Ridge National Laboratory
Oak Ridge, TN 37831-6068

W. Westphal and F. Macri
Rolls-Royce Allison
Indianapolis, IN 46206-0420

ABSTRACT

This paper provides a review of recent studies undertaken to examine the mechanical and thermal stability of silicon nitride ceramic vanes with and without an oxide-based environmental barrier coating (EBC) after field tests in an industrial gas turbine. Two commercially available silicon nitride vanes (i.e., AS800 and SN282) were evaluated, where the AS800 vanes had an EBC and the SN282 vanes did not. The average temperature and pressure of gas impinging upon the vanes were approximately 1066°C and 8.9 atm, respectively. Both silicon nitride vanes were subjected to exposure time up to 1818h. Scanning electron microscopy was used to provide an insight into the changes in the microstructures of silicon nitrides and EBC arising from the environmental effects. The recession of the airfoils resulting from the volatilization of the normally protective silica layer, and /or EBC, was also measured using a coordinate measuring machine. The long-term chemical as well as structural stability of the secondary phases as well as EBC were characterized using x-ray diffraction. The surface strength of exposed airfoils was evaluated using a miniature biaxial test specimen, which was prepared by a diamond core drilling.

INTRODUCTION

High performance silicon nitride (Si_3N_4) and silicon carbide (SiC) ceramics are leading candidates for applications as high-temperature structural components in advanced gas turbines [1-5]. These materials offer the advantages of (1) low density, (2) refractoriness, (3) adequate short-term strength, and (4) good corrosion and oxidation resistance at intermediate to high oxygen partial pressures over their metallic counterparts.

Recent ceramic gas turbine programs at both Rolls Royce Allison and Solar Turbines [6-8] have done much to increase the experience base concerning the behavior of ceramic components in industrial gas turbines. A key lesson learned in both programs is that environmental effects may severely limit the long-term reliability and performance of silicon-based structural components. In particular, the high gas velocities and the presence of high-temperature, high-pressure water vapor in the environment can lead to the volatilization of the normally protective silica layer. Researchers at NASA Glenn Research Center [9-11] have shown that the presence of water vapor leads to the formation of a gaseous $Si(OH)_4$ species via a reaction with the silica layer. The rate of formation, k, of this species and, thus the rate at which the SiC (or Si_3N_4) is consumed by its continued oxidation, is determined by the expression,

$$k \quad v^{1/2}\, P(H_2O)^2/(P_{total})^{1/2} \qquad (1)$$

where v is the gas velocity, $P(H_2O)$ is the partial pressure of the water vapor, and P_{total} is the total pressure. For lean burn conditions, k for a number of SiC based materials is found to be well described by the expression,

$$k\ (mg/cm^2\ h) = 2.04 \exp(-108\ kJ/mole/RT)\ v^{1/2}\ P_{total}^{3/2} \qquad (2)$$

where T is the absolute temperature (K), v is m/s, and P is atm. In addition to the volatility issues, which may lead to loss of function due to excessive changes in component dimensions, the effect of the environment upon the mechanical stability must be addressed as well.

Recently Rolls Royce Allison successfully carried out a field test on uncoated AS800 silicon nitride vanes [12, 13]. The uncoated AS800 vanes were exposed in an Allison Model 501-K turbine for 815 h, which included a 22 h shakedown test. Results

Copyright © 2002 by ASME

of detailed characterization on the exposed vanes indicated that AS800 vanes exhibited a significant material recession and the rate of which appeared to be controlled by the subjected local temperature. It was concluded that the lifetime of the uncoated AS800 vanes was controlled by dimensional and not mechanical considerations. It was, therefore, suggested that environmental barrier coatings would be required to reduce the recession rates of silicon nitride components to acceptable levels within the expected operational lifetime.

This paper describes the results of a recent component verification effort involving silicon nitride vanes with and without EBC exposed in an industrial gas turbine. The surface strength as a function of exposure time was measured using a miniature biaxial specimen, which was prepared by diamond core drilling. Scanning electron microscopy was used to elucidate the changes in the microstructures arising from the oxidation process in turbine environments. The stability of the secondary phases was evaluated using x-ray diffraction.

EXPERIMENTAL PROCEDURE

Materials

The vanes examined in this engine field test were fabricated from either AS800 (Honeywell Ceramic Components, Torrance, CA) or SN282 (Kyocera Industrial Ceramics Corp., Vancouver, WA) silicon nitride. Both materials, which are densified by gas pressure sintering using rare-earth sintering aids, are classified as self-reinforced silicon nitride ceramics due the development of whisker-like β-silicon nitride grains. The crystalline phases in the as-received materials are β-Si_3N_4 and a modified H-phase ($Sr_2La_4Y_4(SiO_4)_6O_2$) for the AS800 and β-Si_3N_4, $Lu_2Si_2O_7$, and Lu_2SiO_5 for the SN282. The AS800 vanes were tested with an oxide-based EBC, while the SN282 vanes were not. The EBC system evaluated in the present program was an experimental plasma-sprayed oxide (PSO) provided by Honeywell Ceramic Components and applied directly to the AS800 vanes without a bond coat.

Engine Tests

The first stage ceramic vanes (Fig. 1) were designed for retrofit into a Model 501-K turbine (Rolls-Royce, Indianapolis, IN). The vane assembly was mounted in a Model 501-K turbine at a commercial site (Exxon - Mobile, AL). During the engine field test at Exxon, the average temperature and pressure of gas entering the vanes were approximately 1066°C (1950°F) and 8.9 atm (128 psia), respectively. However, due to the combustor temperature pattern, the mid-span gas temperature could have been as high as 1260°C (2300°F) at the "hot spot". The inlet gas velocity at vane midspan was about 162 m/s (530 ft/sec) and the gas accelerated to about 573 m/s (1880 ft/sec) at the vane exit. Due to the extremely humid conditions during the engine test, the mole fraction of water vapor for the gas entering the vanes was calculated to be 0.101.

The engine sustained power and maintained performance throughout operation. It was subjected to the rigors of commercial operation including emergency shutdown (highest stress condition) and full power water wash in the Phase I testing [13]. In the Phase II testing, no engine washes were conducted. The engine was periodically shutdown for pre-planned inspections and removal/replacement of selected vanes for subsequent component evaluations. Table 1 summarizes the vanes removed for examination during the field test.

Vanes Characterization

The first characterization method involved dimensional inspection of the vanes removed during the periodic field inspections. As indicated in Table 1 selected vanes were dimensionally inspected with a coordinate measuring machine (CMM). Here the primary emphasis was to measure changes in the shape of the midspan slice of the airfoil as a function of engine test time. A limited number of profiles were also taken along the trailing edge region (Fig. 1a).

X-ray diffraction was used to identify the predominant secondary phase(s) in the airfoil as a function of engine test time. For each airfoil examined, diffraction patterns were obtained for the platform surface as well as the convex and concave sides of the airfoil. Scanning electron microscopy (SEM) was first used to examine the surfaces of the airfoils and platforms after removal of the vanes from the engine. Selected vanes were subsequently sectioned by making a longitudinal cut parallel and adjacent to the trailing edge (Fig. 1a). These pieces were subsequently polished and examined with SEM to provide an insight into the effect of the turbine environment on the long-term stability of the microstructure and chemistry of both silicon nitride ceramic vanes and the employed EBC.

The biaxial flexure strength [14-16] was measured for selected vanes using a ball-on-ring arrangement. Specimens were machined from both the airfoil and platform surfaces by first diamond core drilling small cylinders having nominal diameters of 6.0 mm. Each cylinder was then machined on one face only until the thickness was 0.4 to 0.5 mm. In this way one face of each specimen always consisted of the exposed surface of either the airfoil or platform. During testing, the exposed surface was loaded in tension.

The test fixture consisted of a 1 mm diameter WC ball, which was mounted to a miniature load cell. The lower support ring, which was 5.0 mm in diameter, was fabricated from a high-strength polymer. The test fixture was mounted to a vertical stepper motor (Z stage), which was affixed to the X-Y stages for positioning in the horizontal plane. A personal computer controlled all three stages. After placing a specimen on the lower support ring, the X-Y stages were used to position the assembly directly under the upper load ball. The Z-stage was then raised at a rate of 0.5 mm/s until the specimen made a light contact with the ball. The specimen was subsequently loaded to failure at a displacement rate of 0.05 mm/s. The computer monitored and recorded the

Copyright © 2002 by ASME

displacement, load, and time.

The strength, S_b, was calculated from the equation

$$S_b = 3P(1+n)/(4nt^2)\bullet[1 + 2\ln(a/b) + ((1-n)/(1+n))(1 - b^2/2a^2)(a^2/R^2)] \quad (3)$$

where P is the ultimate sustained load, a is the radius of the support ring, b is the effective radius of contact of the loading ball on the specimen, R is the specimen radius, t is the specimen thickness, and n is Poisson's ratio. As a first approximation, b was taken as t/3.

RESULTS AND DISCUSSION

Uncoated SN282 Vanes

Observations of periodic field inspections indicated that the material behavior of the uncoated SN282 vanes during the present field tests was similar to that of the uncoated AS800 vanes employed in a previous engine field test [12]. For example after only 200h, a light colored phase appeared on the outer airfoil surfaces. SEM analysis of exposed airfoil surface indicated that this deposit had a composition identical to that of the secondary phase of the SN282 implying that the silicon nitride grains had been removed as a consequence of material recession. The presence of this light colored phase on the airfoils became more prominent with an increase of engine test time. Subsequent x-ray analysis further confirmed that the light color deposit on airfoil surfaces exhibited a phase of $Lu_2Si_2O_7$.

The CMM data obtained were used to measure the airfoil thickness in both the leading and trailing edge region. Results of CMM for the midspan region confirmed that the profile of 200h test vanes was very similar to that measured for the as-received vane. Note that in the previous field test, measurable recession for the uncoated AS800 vanes was not observed until after 200h. However, the progressive material recession with time ultimately led to significant changes in the shape of the airfoil as illustrated in Figure 2 for both the leading edge and the trailing edge region. The excessive loss of material was due to the inability of silicon nitride material to form and retain a protective silica scale, which was swept away by the high velocity gas. The continuously competing processes of silica scale formation and volatilization eventually led to a steady-state value of the scale thickness as well as a linear recession of the silicon nitride substrate.

Figure 3 compares the thickness change in the trailing edge region for the uncoated SN282 and uncoated AS800 vanes reported previously [12]. Although the average material loss rates were similar for both silicon nitrides, the scatter in the SN282 data is significantly less. This difference was most likely due to the way in which the measurements were made and not intrinsic material characteristics. Specifically, the use of a micrometer for the uncoated AS800 measurements in the previous field test (versus a CMM for the SN282) would be expected to lead to greater position errors and thus an increased uncertainty in the thickness value. Given that the underlying recession process (oxidation of the silicon nitride and volatilization of the resulting silica scale) was identical for both materials, one would expect that the trends in the thickness change versus time data should be comparable in spite of the differences in secondary phase microstructure and chemistry.

SEM examinations of the polished cross-sections revealed that the microstructure of the SN282 vanes was stable with time (Fig. 4). Note that the micrograph after field test illustrates the accumulation of the secondary phase on the surface due to the loss of silicon nitride by environmentally induced recession and, no apparent change in the microstructure of the silicon nitride substrate. This material recession could have also been responsible for the slight increase in surface roughness with time. Note that for the uncoated AS800 vanes in the previous field test, there was a significant increase in the extent of development of subsurface damage zone, i.e., intergranular cracking and dissociation of the silicon nitride grains. Thus, one can conclude that uncoated SN282 exhibits a relatively more stable microstructure in a gas turbine environment, which could be attributed to the stability of its secondary phase.

The strength data of uncoated SN282 vanes after field tests are shown in Figure 5. Results showed that the strength of SN282 biaxial specimens machined from the airfoil surfaces did not change appreciably with time, similar to those previously reported for the uncoated AS800 vanes [12]. Also, results of limited data of samples from platform regions, which were subjected to low temperatures during field tests, indicated that the strength from airfoil region was comparable to that obtained from platform region. There was, however, a tendency for the standard deviation to increase with time due in part to the increased occurrence of low strength specimens resulting from the increased surface roughness (flaw size). The results for the uncoated SN282 and uncoated AS800 vanes suggested that the time-dependent strength degradation was not of a primary concern for component performance. Instead one would expect that the ultimate loss of component function could result from material recession, and thus loss of load-bearing capability. To estimate the effect of this process, the CMM data were used to calculate the cross-sectional area of the midspan region as a function of time. Results showed that the cross-sectional area of the uncoated SN282 vanes was reduced by approximately 27% after 1818h engine test. As a first approximation, the decrease in cross section should result in a significant increase in the subjected stress levels during operation.

Coated AS800 Vanes

The periodic field inspections found out that a number of the Honeywell PSO coated AS800 vanes experienced debonding and spallation during the field test (see Table 1). In general, the coating spalled along the midspan airfoil region where the temperature and gas velocity level was the highest. Also, the coated AS800 vanes, located at the hot-spot region of engine, were

Copyright © 2002 by ASME

frequently observed to have more coating spallation as compared to those located outside the hot-spot regions. Observations also showed that a light colored scale, identified as the modified H-phase via x-ray and SEM analysis, began to appear on the airfoil surfaces after the spallation of PSO EBC. The presence of the light colored secondary phase deposit again was due to the oxidation and volatilization of silicon nitride.

The CMM data obtained in the current field test were used to evaluate the change in thickness of the trailing edge regions of the coated AS800. Fig. 6 compares the thickness change for the coated AS800 vanes in the present field test and the uncoated AS800 vanes in the previous filed test as a function of engine test time [12]. The loss of the PSO EBC early in the course of the field test caused the thickness change (thickness reduction) to be significantly larger for the coated AS800 for times less than 600h. However, after the total loss of Honeywell PSO EBC the AS800 substrate should expect to exhibit a similar recession trend to the uncoated vanes as shown in Fig. 6.

SEM micrographs of the polished cross-sections of the vane midspan leading edge and trailing edge region are shown in Fig. 7. The disappearance of the Honeywell PSO coating with time was, in part, due to spallation of the coating as described above. The fact that the coating spalled during biaxial disk specimen fabrication (even on as-received coated vanes) indicated that the coating was weakly bonded to the AS800 substrate. There was also a tendency for the PSO EBC to gradually thin in several regions along the midspan airfoil surface. However, it was difficult to quantify the recession of Honeywell PSO EBC as a function of time due to the fact that the original coating thickness was not uniform. Closer observation of the coating surface revealed the formation of a columnar-like structure due possibly to the phase instability of PSO in the presence of the turbine environment (Fig. 8). However, X-ray diffraction results were not conclusive.

Even in those cases where the Honeywell PSO remained intact, extensive silica formed due to the oxidation of silicon nitride underneath the coating (Fig. 9a). A subsurface damage zone, consisting of partially oxidized silicon nitride grains, cracking between the silicon nitride grains, and a change in the microstructure of the secondary phase, was also observed for PSO coated AS800 (Fig. 9b). The extent of this subsurface damage zone developed varied from location to location along the airfoil. However, the depth of the environmentally induced damage zone on the pressured side was, in general, greater than that developed on the suction side. As result, it was likely that once the PSO EBC spalled, this damage zone was quite susceptible to fracture. This explains the very rough surfaces observed in the leading edge profiles (1818 h vane in Fig. 7c) and thus very low strength as described below.

The strength data for the PSO coated AS800 (airfoil surface) are shown in Fig. 10. As indicated previously, the preparation of these specimens always resulted in spallation of the Honeywell PSO EBC. In many cases, the spallation resulted in the formation of a very rough tensile surface particularly for those airfoils that had been subjected to long field exposures. As a result, the resulting strength values were quite low compared to those generated for the uncoated AS800 (Fig. 10). The standard deviation was quite high due to the existence of a few low strength specimens. The specimens with low strength could be also attributed to the development of a large subsurface damage zone (silica plus intergranular cracking) induced by the turbine environment.

Results of the present field test suggested that the experimental Honeywell PSO EBC was not an effective diffusion barrier for water vapor to reach the silicon nitride substrate. It did, nonetheless, limit the loss of material by volatilization. However, the microstructure of the AS800 underneath the Honeywell PSO EBC exhibited a significant subsurface damage zone, silica plus intergranular cracking, which was very similar to those observed in a previous study [17] involving exposure of the various silicon nitrides to a high-temperature, high-pressure water vapor environment. Note that the previous study did not include high velocity gas flow, and thus the volatility effects were insignificant. The presence of this subsurface damage zone could significantly reduce the load bearing capability and long-term reliability of components

SUMMARY

Both uncoated SN282 and PSO coated AS800 silicon nitride vanes were successfully exposed in a commercial gas turbine for up to 1818 h. Analysis of x-ray diffraction and SEM indicated that the microstructure and intergranular phase composition were stable with time. However, both uncoated SN282 and PSO coated AS800 vanes did experience significant material recession, the rate of which appeared to be controlled by temperature and to a minor extent upon the sintering additives. Results also indicated that the experimental Honeywell PSO EBC system employed in the present engine tests did not provide an adequate protection (diffusion barrier) from gas turbine environments. Thus, the PSO coated AS800 vanes exhibited similar recession rate and materials degradation to those uncoated AS800 vanes evaluated in a previous engine test. Finally the strength measured for biaxial disks machined from the uncoated SN282 airfoil surfaces did not change significantly with time. On the other hand, the strength of samples machined from PSO coated AS800 airfoil surfaces decreased with an increase in exposure time due to the formation of a very rough surface and/or subsurface damage zone. These observations indicate that the lifetime of the silicon nitride vanes is controlled by dimensional and not mechanical considerations. Therefore, alternative EBC systems need to be explored and developed to inhibit material recession and ensure a long-term stability and performance in gas turbine environments.

Copyright © 2002 by ASME

ACKNOWLEDGEMENTS

The authors thank Drs. C.H. Hsueh, J. A. Haynes, and P. F. Becher for reviewing the manuscript. Research is sponsored by U.S. DOE, Office of Power Technologies, Microturbine Materials Program, under Contract DE-AC05-00OR22725 with UT-Battllee, LLC.

REFERENCES

[1] Anson, D., Ramesh, K. S., and DeCorso, M., "Application of Ceramics To Industrial Gas Turbines"; Volume 1 Technology Background; Volume 2 Economics, Market Analysis, and R&D Plan DOE/CE/40878-1&2; Battelle Columbus March 1991.

[2] Helms, H. E., Johnson, R. A., and Groseclose, L. E., "AGT 100-Advanced Gas Turbine Technology Development Project," pp. 137-55 in Proceedings of the Twenty-Third Automotive Technology Development Contractors' Coordination Meeting, P-165, Society of Automotive Engineers, Warrendale, PA, March 1986.

[3] van Roode, M., "Ceramic Retrofit Program," pp. 77-93 in Proceedings of the Joint Contractors Meeting: FE/EE Advanced Turbine Systems Conference FE Fuel Cells and Coal-Fired Heat Engines Conference, DOE/METC-93/6132, August 1993.

[4] Carruthers D., and Lindberg, L., "Critical Issues for Ceramics for Gas Turbines," pp 1258-1272 in Third International Symposium on Ceramic Components and Materials for Engines, edited by V. J. Tennery, American Ceramic Society, Westerville, Ohio, 1988.

[5] Haley, P. J., Holtman, R. L., Groseclose, L. E., Hilpisch, S. J., and Bell III, A. H. "Advanced Turbine Technology Applications Project (ATTAP)", pp 19-29 in Proceedings of the Twenty-Ninth Automotive Technology Development Contractors' Coordination Meeting, Society of Automotive Engineers, Warrendale, Penn., June 1992.

[6] van Roode, M, Brentnall, W.D., Smith, K.O., Edwards, B.D., Faulder, L.J., and Norton, P.F., "Ceramic Stationary Gas Turbine Development - Third Annual Summary", ASME Paper 96-GT-460, presented at the International Gas Turbine and Aeroengine Congress and Exposition, Birmingham, U.K., June 10-13,1996.

[7] Parthasarathy, V., van Roode, M., Price, J., Gates, S., Waslo, S., and Hoffman, P., "Review of Solar's Ceramic Stationary Gas Turbine Development Program, Proceedings of the 6th International Symposium on Ceramic Materials and Components for Engines, Arita, Japan, October 19-23, 1997. pp. 259-264, 1997.

[8] Wenglarz, R., Ali, S., and Layne, A., "Ceramics for ATS Industrial Turbines," to be published in the proceedings of ASME Turbo Expo '96 Conference, Birmingham, UK, June 10-13, 1996.

[10] Opila, E. J. and Hann, Jr., R. E., "Paralinear Oxidation of SiC in Water Vapor, "*Journal American Ceramic Society*, Vol. 80, No. 1,

[11] Smialek, J. L., Robinson, R. C., Opila, E. J., Fox, D. S., and pp. 259-264, 1997.

[9] Opila, E. J., "Variation of the Oxidation Rate of SiC in Water Vapor, " *Journal American Ceramic Society*, Vol. 82, No. 3, pp. 625-36 (1999).

Jacobson, N., "SiC and Si_3N_4 Recession due to SiO_2 Scale Volatility Under Combustor Conditions, " *Advanced Composite Materials*, Vol. 8, No. 1, pp. 33-45, (1999).

[12] Ferber, M. K., Lin, H. T., Parthasarathy, V., and Wenglarz, R. A., "Characterization of Silicon Nitride Vanes Following Exposure in an Industrial Gas Turbine," presented at IGTI Meeting in Munich, Germany, May 2000; and published as an ASME 2000-GT-631 pamphlet.

[13] Wenglarz, R. A. and Kouns, K., "Ceramic Vanes for a Model 501-K Industirla Turbine Demonstration," presented at IGTI Meeting in Munich, Germany, May 2000; and published as an ASME 200-GT-73 pamphlet.

[14] Kirstein, A. F. and Woolley, R. M., "Symmetrical Bending of Thin Circular Elastic Plates on Equally Spaced Point Supports," *Journal of Research of the National Bureau of Standards - C. Engineering and Instrumentation*, Vol 71C, No 1, Jan-Mar 1967.

[15] Thiruvengadaswamy, R. and Scattergood, R. O., "Biaxial Flexure Testing of Brittle Materials," *Scripta Metall. et Mater.*, Vol 25, 1991, pp2529-2532.

[16] Shetty, D. K., Rosenfield, A. R., McGuire, P., Bansal, B. K., and Duckworth, W. H., "Biaxial Flexure Tests for Ceramics," *Ceramic Bulletin*, Vol 59, No 12, 1980, pp 1193-97.

[17] Ferber, M. K., Lin, H. T., and Keiser, J., "Oxidation Behavior of Non-Oxide Ceramics in a High-Pressure, High-Temperature Steam Environment," *Mechanical, Thermal and Environmental Testing and Performance of Ceramic Composites and Components, ASTM STP 1392*, M. G. Jenkins, E. Lara-Curzio and S. T. Gonczy, Eds., American Society for Testing and Materials, West Conshohocken, PA, 2000.

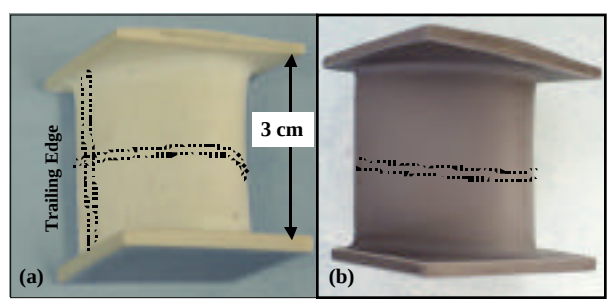

Figure 1. Photographs of as-received silicon nitride vanes prior to field testing. (a) AS800 vane coated with an experimental PSO EBC and (b) uncoated SN282. The dotted lines show the sections that were machined for subsequent polishing and evaluation by scanning electron microscopy.

Copyright © 2002 by ASME

Table 1: Silicon nitride vanes selected for component characterization. Note that (K) and (H) refer to SN282 and AS800 vanes, respectively. L.E. denotes leading edge and T.E. denotes trailing edge region of airfoil.

Time (h)	Vane No	EBC	comments	Characterization
0	14 (K)	none	intact	CMM, Microscopy, X-Ray
0	162 (H)	Honeywell PSO	intact	CMM, Microscopy, X-Ray
200	48 (K)	none	no distress	CMM, Microscopy, X-Ray
200	129 (H)	Honeywell PSO	bubbling of coating along pitch line, both surfaces	Microscopy, IR Imaging, X-Ray
200	168 (H)	Honeywell PSO	no distress	CMM, Microscopy, IR Imaging
524	122 (H)	Honeywell PSO	spalled to 60% from T.E. forward on suction surface, L.E. loss	CMM, Microscopy, X-Ray
524	131 (H)	Honeywell PSO	spalled from T.E. 30% forward on pressure surface, 40% of span about pitch line on suction surface	CMM, Microscopy, X-Ray
524	145 (H)	Honeywell PSO	loss on L.E., .08” wide	CMM
624	45 (K)	none	s/n 00045 (k) slight L.E. and ~50% T.E. on pressure side erosion	CMM, Microscopy
624	15 (K)	none	s/n 00015 (k) light local scoring on outer T.E.	CMM, Microscopy
624	19 (K)	none	s/n 00019 (k) good condition	CMM
624	153 (H)	Honeywell PSO	s/n 153 (h) good condition	CMM, Microscopy
624	152 (H)	Honeywell PSO	s/n 152 (h) broken in engine	Microscopy
624	166 (H)	Honeywell PSO	s/n 166 (h) good condition	CMM, Microscopy
624	137 (H)	Honeywell PSO	s/n 137 (h) L.E. and T.E.spallation, L.E. erosion	CMM, Microscopy
1148	17 (K)	none	chipped corner	CMM
1148	32 (K)	none	some pitch line loss (~50% span) both pressure and suction surfaces	CMM, Microscopy, X-Ray
1148	39 (K)	none	chipped corner	CMM
1148	47 (K)	none	chipped corner	CMM, Microscopy
1148	96 (H)	Honeywell	good condition	CMM, Microscopy, X-Ray
1621	101 (H)	Honeywell PSO		CMM
1621	108 (H)	Honeywell PSO		
1621	110 (H)	Honeywell PSO		CMM
1621	120 (H)	Honeywell PSO		
1621	123 (H)	Honeywell PSO		CMM, Microscopy, X-Ray
1621	133 (H)	Honeywell PSO		CMM

Copyright © 2002 by ASME

Table 1. (continued)

Time (h)	Vane No	EBC	comments	Characterization
1818	25 (K)	none		CMM
1818	26 (K)	none		CMM, Microscopy, X-Ray
1818	28 (K)	none		
1818	158 (H)	Honeywell PSO		
1818	163 (H)	Honeywell PSO		

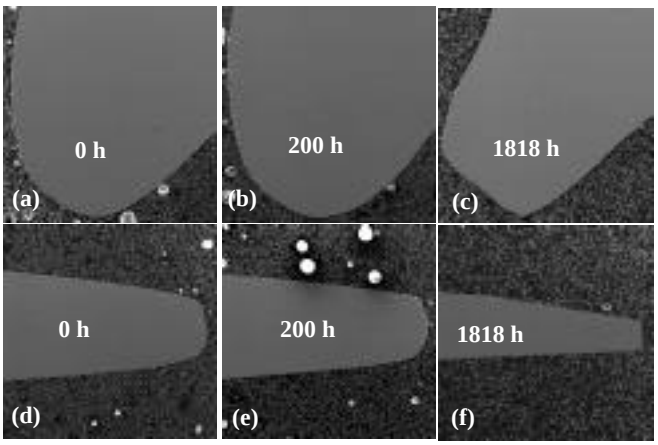

Figure 2: SEM micrographs of leading edge (a, b, and c) and trailing edge (d, e, and f) midspan profiles of uncoated SN282vanes showing effect of engine test time upon the shape of airfoil.

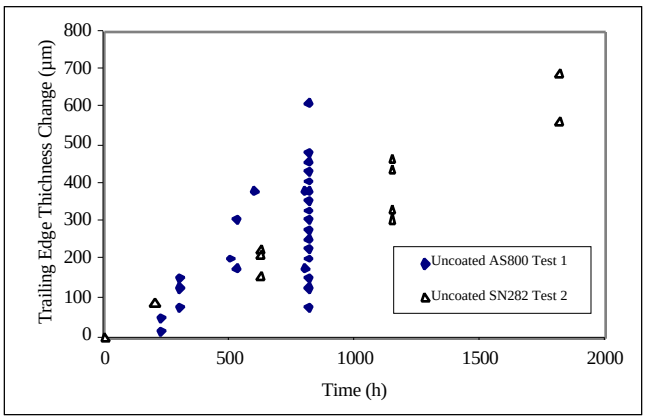

Figure 3: Comparison of trailing edge thickness values for uncoated SN282 (present field test, Test 2) and uncoated AS800 (previous field test, Test 1) as a function of engine test time.

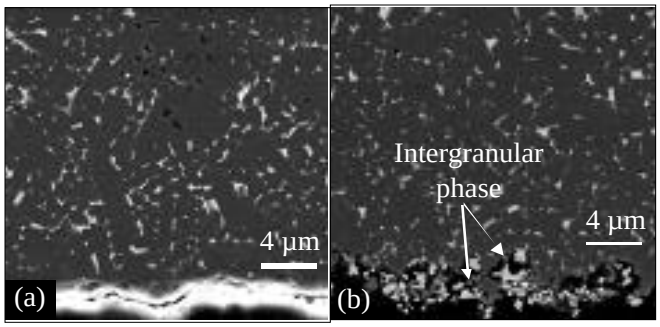

Figure 4: Comparison of typical microstructures of the polished cross section of uncoated SN282 vanes at (a) as-received and (b) after 1148 h field test condition.

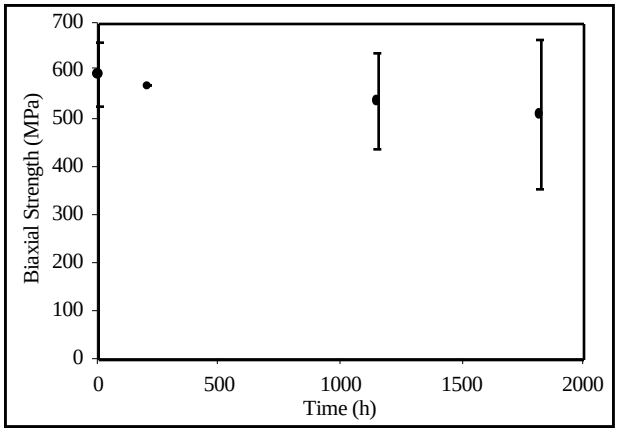

Figure 5. Biaxial strength data of airfoil surfaces as a function of engine test time for uncoated SN282 vanes.

Copyright © 2002 by ASME

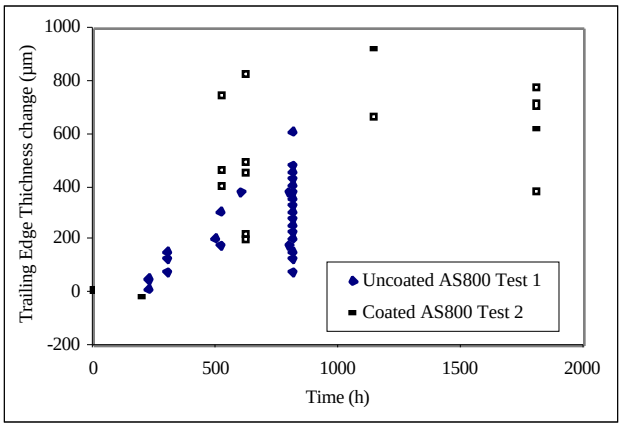

Figure 6. Comparison of trailing edge thickness values for PSO EBC coated AS800 vanes (present field test, Test 2) and uncoated AS800 (previous field test, Test 1) as a function of engine test time.

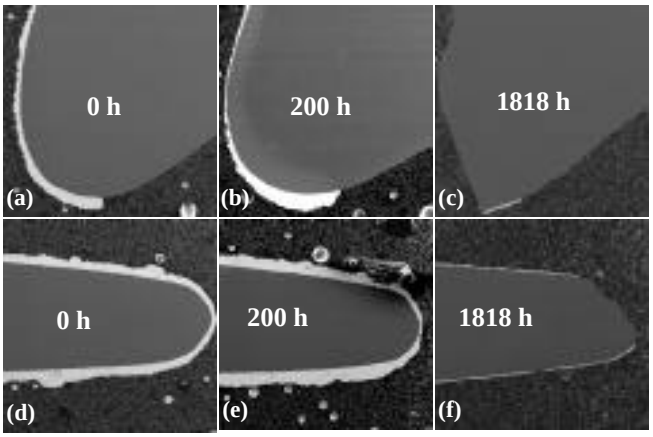

Figure 7: SEM micrographs of leading edge (a, b, and c) and trailing edge (d, e, and f) midspan profiles of Honeywell PSO EBC coated AS800 vanes showing effect of engine test time upon the shape of airfoil.

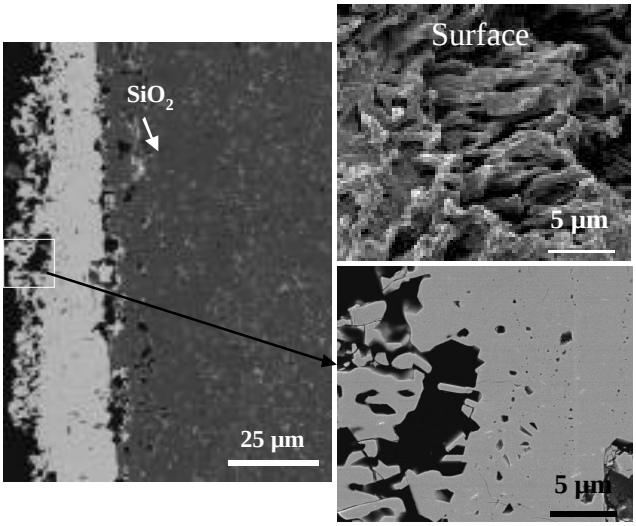

Figure 8: SEM micrographs illustrating the PSO coating morphology in vicinity of trailing edge region of coated AS800 vane (#137 - 624 h filed test).

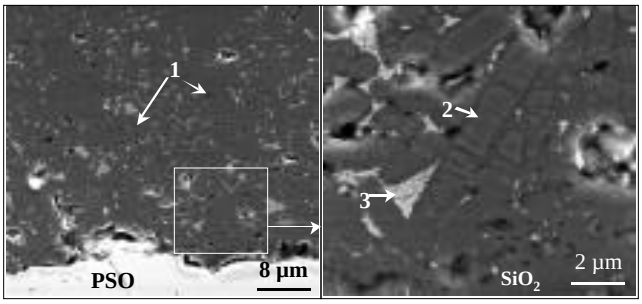

Figure 9: SEM micrographs for Vane 168 (200 h) illustrating the subsurface damage zone in the silicon nitride beneath the Honeywell PSO EBC. 1 denotes the cracking between silicon nitride grains, 2 denotes the oxidation of silicon nitride grain, and 3 denotes the microstructure change in secondary phase.

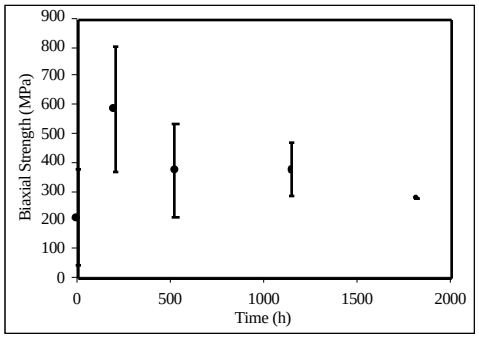

Figure 10. Biaxial strength data of airfoil surfaces as a function of engine test time for Honeywell PSO coated AS800 silicon nitride vanes.

Copyright © 2002 by ASME